The composition of edible oils modifies β-sitosterol/γ-oryzanol oleogels part II: Addition of selected minor oil components

Authors:
Maria Scharfe, Daniel Prange, Eckhard Flöter
Department of Food Processing, Technical University Berlin, Berlin, Germany

Corresponding author:
Maria Scharfe,
Seestrasse 13, 13353 Berlin, Germany
+493031427588
maria.scharfe@tu-berlin.de

Abstract
The first part of this study showed that the triglyceride composition of purified oils has little impact on sterol/sterol ester oleogels. Hence, changes in the gels' properties observed in previous studies must arise from minor polar components, particularly by changing the interactions within the fibrillar network. Selected molecules (oleic acid, tocopheryl acetate, monoglycerides, and water) were added to three purified oils to unravel the individual contributions introduced by different functional groups. While all additives retarded the molecular self-assembly of sitosterol with oryzanol, distinct effects were found for gel hardness, transition temperatures and enthalpies, strain sweep responses, and microstructure. It was discovered that the maximum storage modulus in the linear viscoelastic region does not necessarily relate to the gels' compression firmness. In samples comprising oleic acid and tocopheryl acetate, discrete interaction mechanisms with the scaffolding elements were suggested since results between the two additives developed differently and were dose-dependent. A network supporting effect was suggested at low concentrations, in line with previous results for oils comprising low levels of thermal deterioration products. The microstructure of oleogels was considerably modified with additives. Unfortunately, effects are difficult to quantify due to the packed surface observed in AFM micrographs.

1. Introduction
The first part of this study provided necessary information about the oil sterol/sterol ester oil structuring system and addressed the role of the fatty acid (FA) composition of triglycerides (TAGs) [1]. The results showed that this variable had little effect on the oleogels. Nevertheless, minor effects such as a drift in gel-sol transition temperature, different network arrangements, and firmness were observed. However, compared to the influence of minor polar components reported in earlier studies, these effects seem negligible [3–6]. This introduction will discuss minor polar components' influence on the gels concerning potential disruptions in the regular molecular network interactions, determining the gels' macroscopic properties. Therefore, potential interaction points in the network will be discussed, and relevant literature addressing this issue will be reviewed.
The development of the primary network building blocks addressed either as tubules, tubes, or fibrils is based on the molecular stacking of the sterol and the sterol ester through hydrogen bonds formed between the hydroxyl groups of sitosterol and the carbonyl groups of oryzanol (Figure 1). The free energy of binding (ΔG) is negative (-23.2 kJ/mol); hence the dimer formation is energetically favored [7, 8]. Interestingly, the hydrogen bond contributes little to the free energy of binding within the tube (-2.3 kJ/mol), which is predominately assigned to van der Waals forces (vdW) and desolvation energy. Nevertheless, it allows for a parallel alignment of the sterane cores while the methyl groups of oryzanol at C4 and C14 enable for a slightly tilted stacking resulting in the wedged-shaped fibril [8, 9]. Although

the hydrogen bond is relatively stable, the strength of the fibril structure mainly builds on π-π contacts between the aromatic groups of oryzanol, which form a network of non-covalent supportive interactions. The potential binding enthalpy of the dimer was found to be approximately -8.7 kJ/mol, indicating that

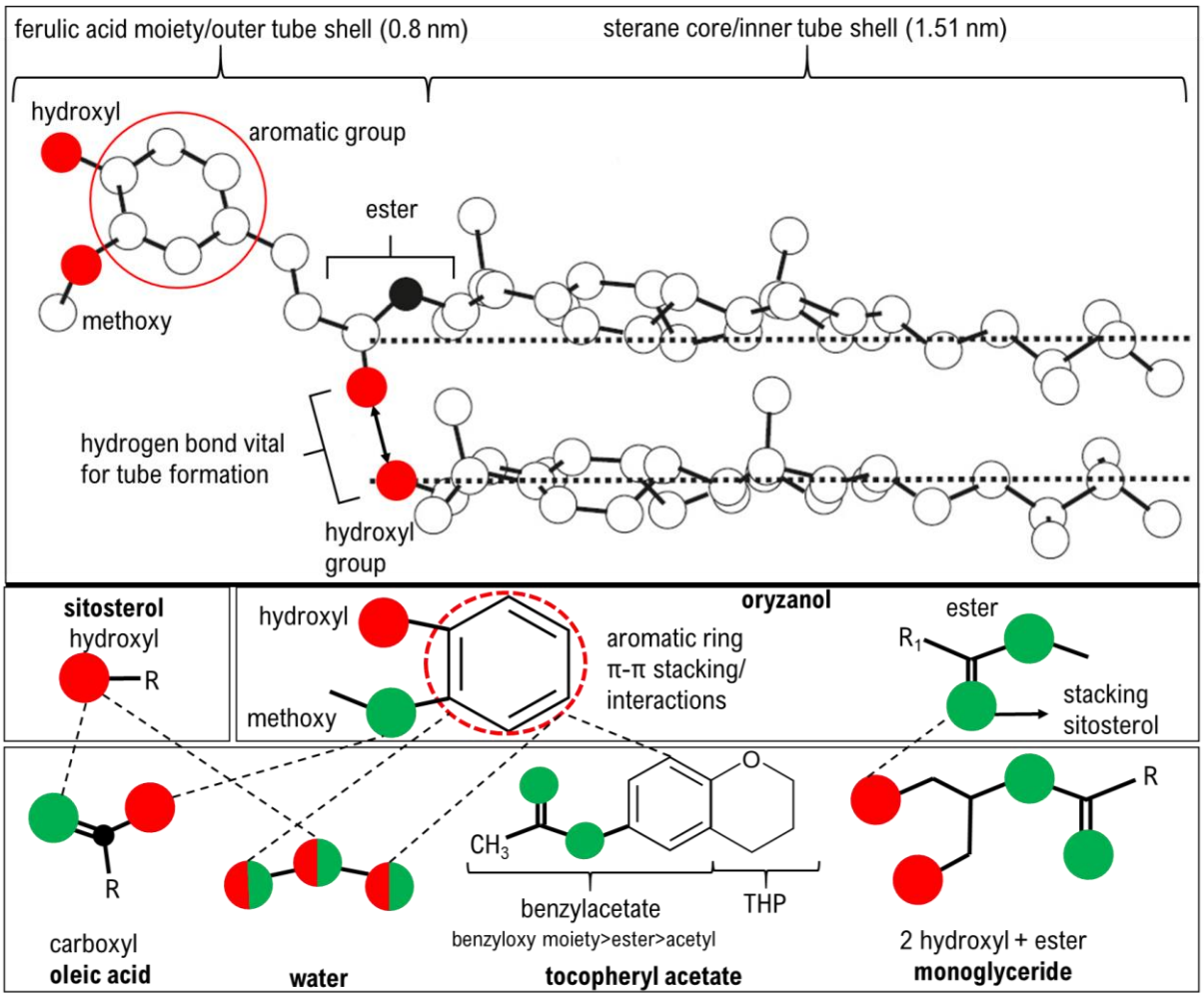

Figure 1 Top: stacking of γ-oryzanoland β-sitosterol, red indicates main interactions points which contribute to the stability of the tube or form inter-fibril interactions, modified with permission from Bot and Flöter (AOCS Press) [2], bottom: potential interactions of additives' functional groups with functional groups of sitosterol and oryzanol, red cicles: hydrogen bond donor, green circles: hydrogen bond acceptor, red dotted line: π-π interactions and aromatic stacking, graphic does not aim to provide complete overview of all possible interactions

the process is enthalpy-driven [7, 8]. However, the binding enthalpy appears to depend on the type of solvent so that ΔG decreases with oil polarity [7]. Hence tubes are more stable in solvents with a lower polarity. Molecular dynamics (MD) simulations showed that decane interacted with the sterol and sterol ester molecules throughout the self-assembling process simulation[8]. Similarly, MD simulations showed that glycerol forms hydrogen with the hydroxyl group of the sitosterol and the methoxy, phenol, and carbonyl groups of the oryzanol, enhancing the tubes' stability [4]. However, glycerol reportedly disrupts inter-fibril interactions and thus network formation so that any generated stability is cancelled out. That implies that more polar solvents or polar molecules dissolved in a non-polar solvent potentially interact with the interaction points (Figure 1, red areas) of the structurants, retarding the dimer formation by competitive bonds. That is in line with the observed decrease in sol-gel transition temperatures reported in oils with increasing levels of minor polar components [3].

However, the formation of fibrils is only the first step of oleogel formation. Reportedly, they must aggregate into a three-dimensional network to immobilize the solvent [6]. Interestingly, the same interactions, namely π−π contacts and vdW interactions (aromatic ring and methoxy group) through their ferulic acid moieties, are responsible for fibril formation and fibril aggregation [8]. Hence, there is a shift from intra- to inter-tube interactions when tubes mesh. Besides, hydrogen bonds between the

hydroxyl groups add to the stability. The results obtained by MD simulations were confirmed by distinct peaks of the aromatic ring and methoxy group in the Raman spectra [8].
Considering the interactions discussed, it is fair to assume that the self-assembling process and the aggregation of tubes is disturbed or modified in the presence of molecules able to engage in the type of bonds operational in structure formation. In addition to the shift in sol-gel transition temperatures, modifications of fibrillar bundling are likely if polar molecules accumulate in the proximity of the ferulic acid moieties. That potentially modifies the macroscopic properties of oleogels as well. Whether polar molecules act as inhibitors or promoters of network stability probably depends on their concentration and chemical structure, particularly the nature and number of their functional groups.
That is in line with a recent study where dynamic molecular modeling was used to simulate the interactions during the self-assembly of sitosterol/oryzanol in pure triglycerides and triglyceride/glycerol mixtures (ε~46.5) [4]. The authors reported a disruption of established inter-fibril connections in favor of glycerol interacting with the hydroxyl group of sitosterol and the methoxy, phenol, and carbonyl groups of oryzanol. These newly formed bonds enhanced the individual tube's stability (intra-tube). However, the network strength is mainly induced by inter-tube interactions. Still, the storage modulus dropped significantly at 28 % w/w substitutions by glycerol, indicating that the strengthening of individual tubes is compensated by the absence of bundles in the network in the highly polar solvents [4]. Additionally, in highly polar solvents, an increase in oryzanol solubility can be expected. Indeed, a sevenfold increase of solvent permittivity (1.8 to 13.3, hexane to hexanol) resulted in 7.4 times increased oryzanol solubility [10]. That is possibly due to interactions of the ferulic acid moiety with the hydroxyl group of hexanol. Moreover, oryzanol solubility is increased in the presence of lecithin [11]. Here, oryzanol is engaged with the hydrophobic tails of lecithin micelles by hydrogen bonds through its hydroxyl group and the OPO^- group. For sitosterol, no such effects were observed when glycerol was present, since glycerol molecules do not seem to interact with sitosterol in a way that could hamper self-assembly [4].
However, the study only comprised large substitution levels with glycerol levels of 15 to 50 % w/w [4]. Thus, it maintains unresolved if there is a network strengthening effect of glycerol at low substitution levels. In this case, a lower solvent polarity paired with a moderate number of hydrogen bonds might increase the tubes' stability. Nevertheless, MD simulations showed that intra- and potentially inter-fibril interactions rearrange when polar molecules are introduced to the system. Hence, modifications of the network arrangement could occur on a microscopic scale, impacting the macroscopic properties such as gel strength.
Previously, a few studies addressed the role of solvent type on sterol/sterol ester oleogels. In a first approach, decane, limonene, sunflower oil, castor oil, eugenol (listed in ascending permittivity, range: ε=2.0-10.4) were utilized in sitosterol/oryzanol oleogel emulsions (10% water-in-oil) [6]. Supposedly, solvent polarity expressed as dielectric constant (ε) was negatively correlated to emulsion gel firmness, indicating that the solvent type affects the network formation or amount of tubes or both. Moreover, anhydrous oleogels were significantly harder than emulsion, which suggests that water somehow disturbs the system. That was addressed to the crystallization of sitosterol into a mono-hydrate, more pronounced in polar solvents due to better water solubility. That consequently reduces the amount of fibrils in the gel, similar to the effect described for increased oryzanol solubility in more polar solvents. Bot et al. first recognized signals of hydrated sitosterol crystals in x-ray diffraction patterns of oleogel emulsions [12]. Later, other studies showed that structurant concentration and water activity are critical in preventing recrystallization and oleogel collapse [6, 13]. However, lowering the water activity to values below 0.9, e.g., by adding sodium chloride, impedes sterol hydrate occurrence and avoided the accompanying structure loss [6]. Since most foods contain water, that is essential information for product development.
In another study, the same solvents (decane, limonene, sunflower oil, castor oil, eugenol) were utilized to determine the difference in oleogel properties, such as their formation [7]. The authors reported that the network tends to form at higher temperatures and lower structurants concentration in low-polar solvents. Hence, the self-assembling process is promoted, which is likely related to solubility and viscosity effects.
The same authors published another study in which they included SEM images of decane, limonene, sunflower and castor oil, and eugenol-based oleogels [14]. Castor oil and sunflower oil produced the

hardest gels with a network based on reasonably straight but interconnected fibril bundles. They concluded that this arrangement is beneficial concerning the gels' hardness. However, the authors did not contemplate solubility effects due to solvent polarity, nor was the solvent viscosity considered. The viscosity possibly affects the results of compression tests since it affects the flow through the porous network established by the fibril bundles. One can imagine a sponge filled with sunflower oil (η~22mPa·s) and one soaked up with castor oil (η~935-1100mPa·s). Suppose there is a notable contribution of the flow resistance, depending on the stiffness of the 3-D scaffolding. In that case, the gel's resistance to deformation will directly correspond to the continuous phase's viscosity.
Nevertheless, the network arrangement appears to change with solvent composition, identified by SEM, which is acknowledgedly sensitive to artifacts due to the intense sample preparation. Moreover, the data showed that hardness is not related to solvent permittivity when different chemical types of solvents with a great variety in viscosity are used. Hence, it seems unreasonable to draw reliable conclusions from observation when the effects of solubility, viscosity, and polarity of the solvents superimpose.
S. Calligaris et al. studied the impact of oil unsaturation (flaxseed > sunflower > extra virgin olive oil) and viscosity on firmness and gel-sol transition temperatures of sitosterol/oryzanol oleogels [5]. They reported a decline in gel hardness with increasing solvent viscosity assigned to lower molecular mobility of the structurants. Hence, the probability of coinciding during molecular self-assembly (tubule formation) decreases. However, this was not valid for extra virgin olive oil and flaxseed oil since they exhibited almost identical hardnesses, even though their viscosities vary. Interestingly the data showed a maximum in gel hardness when plotted over solvent permittivity.
In a recent study, the role of solvent composition on β-sitosterol/γ-oryzanol oleogels was studied [3]. To this end, the authors determined the impact of oil purification and by-products of thermal oil deterioration due to exposure to 180 °C on oleogel formation, microstructure, and macroscopic properties such as firmness. Oleogel firmness had a maximum when briefly heated oils were used. Purified oils and deteriorated oils showed a lower firmness possibly associated with modified network interactions and

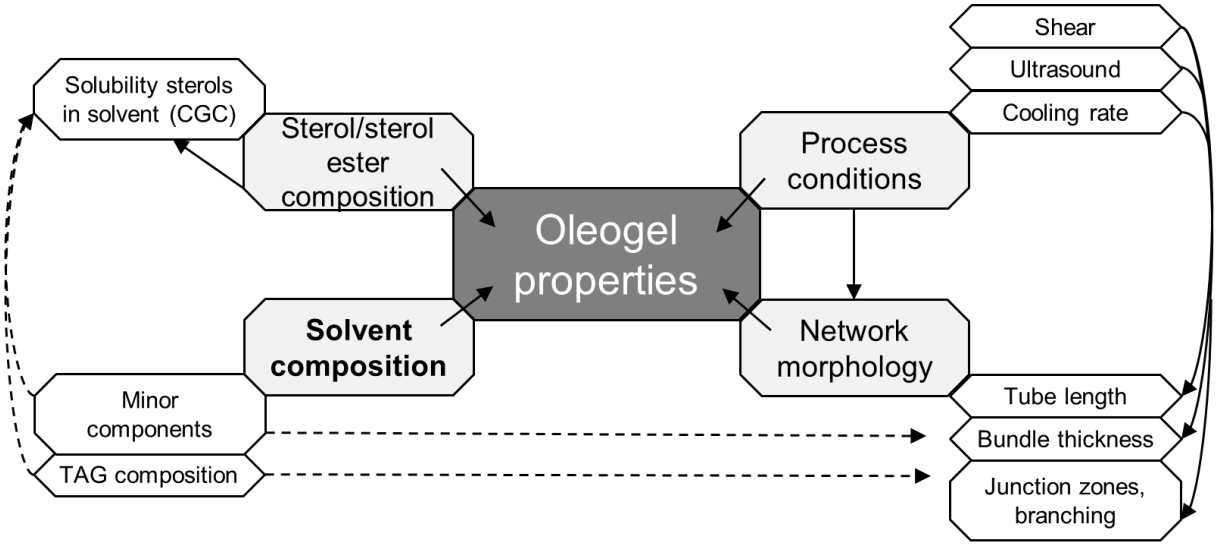

Figure 2 Factors affecting steorl/sterol ester network properties such as compression hardness

thus appearance. The level of polar components progressively suppressed sol-gel transition temperatures due to increased solvent viscosity and interactions of polar molecules with the structurants. In contrast, gel-sol transition temperatures were not considerably affected by the absence (purified oils) or presence of polar components (thermally treated oils). However, in DSC heating thermograms, an asymmetric, prolonged peak (peak fronting) was observed, which indicates that dissolution started at lower temperatures [15]. Interestingly, the enthalpy of dissolution was almost invariable for all samples, while with increasing level of polar components, the peak area decreased, and simultaneously the fronting increased. That suggests that polar components' presence modifies the network's interactions, resulting in a different arrangement of scaffolding elements. Indeed, atomic force microscopy revealed that the bundle arrangement changes dramatically in the presence of polar components.

However, during thermal degradation, numerous species of degradation products are formed. In this study, the intense heating process produced oils that would not be acceptable for utilization in food products. To unravel the contribution of all deterioration species on oleogel properties is impossible. Nevertheless, the study showed that a detailed characterization of oils is necessary to link and compare scientific results dealing with this topic.
Unfortunately, none of the studies discussed above managed to avoid the superimposition of effects contributing to the networks' macroscopic properties (Figure 2). Successful implementations of oleogels are only feasible if there is a holistic understanding of the role of oil composition. Therefore, it is necessary to consider the bulk solvent's contribution (fatty acid profile of TAGs) and the impact of minor polar components separately. Moreover, it is inevitable to utilize a standardized oil for comparability in research.
This study aims to disentangle the contributions of different minor oil components and gain more insight into oleogel formation and properties as the function of solvent characteristics, emphasizing the modification of interactions in the unique sterol/sterol ester system. To this end, minor oil components were removed from three vegetable oils with different degrees of unsaturation (canola< sunflower< flaxseed oil). Representative minor oil components were chosen (oleic acid, tocopheryl acetate, monoglycerides, and water) and admixed to purified oils at different concentrations. Several oil characteristics were recorded before and after the addition. Subsequently, oleogels were produced and tested for their thermal, rheological, and compression behavior. Moreover, the microstructure on the gels' surface was visualized by atomic force microscopy (AFM)

2. Material and methods

Procedures for analysis and sample preparation (except *2.3 Addition of minor components*) remained unchanged to the first part of this study [1]. For practical reasons, they are listed again in this paper.

2.1 Material

For all experiments a phytosterol mix (78.5% β-sitosterol, 10.3% sitostanol, 8.7% campesterol, 0.9% campestanol, Acros, [83-46-5],) and γ-oryzanol (purity > 98%, IMCD 26 Benelux B.V., [11042-64-1]) were used. One should note that sitostanol, campesterol, and campestanol are chemically very similar to β-sitosterol and consequently show similar gelling behavior[16]. Canola oil (Canolin 10770) and sunflower oil (Sonnin 70020) were kindly provided by Walter Rau AG, Neuss, Germany. A 5 l container of flaxseed oil was purchased from Lausitzer Ölmühle Hoyerswerda GmbH (Hoyerswerda, Germany) and used for all experiments. All oils were stored in opaque containers at 3 °C immediately after delivery to prevent deterioration reactions. Oleic acid (technical >90 % oleic acid, max. 8 % linoleic acid) and tocopheryl acetate (>97 %) were purchased from Thermo Fisher GmbH (Kandel, Germany). The monoglyceride mix (Dimodan ® DP MB, >99% monoglycerides) was kindly provided by Danisco (Kopenhagen, Denmark). Table 1 shows the fatty acid composition of the monoglyceride mix.

Table 1 Fatty acid composition of monoglyceride mixture determined via GC according to DGF method C-VI 10a (00)

FA.	**% of total FA**
C 12:0	1.6 ± 0.006
C 16:0	7.5 ± 0.008
C 18:0	63.1 ± 0.015
C 18:1	19.8 ± 0.003
C 18:2	7.5 ± 0.004

2.2 Oil purification

Untreated canola, sunflower, and flaxseed oil were purified by combining the official method for the determination of polar compounds and two methods developed in previous studies [DGF C-III 3b (13)] [17, 18]. Briefly, the oils were mixed with an equal volume of hexane (technical grade, VWR International, Pennsylvania, USA) and subsequently passed a chromatographic column (diameter 20 mm, length 450 mm) packed with a 60 g mixture of activated aluminum oxide (activity grade: Super I, MP Biomedicals) and silica gel (60–200 µm mesh, VWR International) suspended in hexane. The flow through the column was set to 0.4–0.5 ml min^{-1}. The column and the flasks collecting the solution were wrapped in aluminum foil to prevent light-induced oxidation processes. Subsequently, the solvent was removed in a rotary evaporator at 45 °C under vacuum conditions. Traces of hexane were flushed with nitrogen, and the samples were stored at -25 °C before analysis.

2.3 Addition of minor components

Oleic acid, tocopheryl acetate, and a monoglyceride mix were added at total concentrations of 1.0, 2.5, and 5.0 % w/w to all purified oils. The dissolution of monoglycerides at elevated levels (2.5 and 5.0 %) was carried out at 45 °C. 200 ml of each oil were kept in a conditioning cabinet to increase their water content (HPP 260, Memmert GmbH + Co. KG, Schwabach, Germany) at 40 °C and 90 % relative humidity for 48 h. A large absorption surface is beneficial to improve water absorption. Therefore, the samples were poured into glass Petri dishes (Ø 250 mm) and gently mixed 3 times a day. After the addition of minor components, all samples were distributed into small opaque containers (~50 ml) and stored at -25 °C to prevent further reactions. In that way, each test could be performed with a fresh sample.

2.4 Oil analysis

Water content and peroxide value. The water content and peroxide value (PV) of oil samples were determined by titration (Excellence T5, Mettler Toledo, Columbus, USA). The PV was determined according to DGF method C-VI 6a Part 2(02) (Wheeler method). Briefly, 3–5 g oil was diluted in a mixture of chloroform and acetic acid (3:2 v/v, AppliChem GmbH, Darmstadt, Germany). Subsequently, 1 ml of saturated potassium iodate (GPR RECTAPUR, VWR International, Pennsylvania, USA) solution was added. After 180 s at 30 % maximum stirring speed (~300 rpm), 50 ml of deionized water were added. The titration was performed with 10.0 mol $^{-1}$ sodium thiosulfate (Alfa Aesar, Haverhill, USA) and a redox electrode (DMi140-SC, Mettler Toledo, Columbus, USA).
The water content was determined according to DGF C-III 13a (97) (volumetric Karl Fischer method) with a voltammetric electrode (DM143-SC, Mettler Toledo, Columbus, USA). The CombiSolvent Oil Aquastar was used to dissolve about 10 g oil. The titration was carried out using the Combi Solvent Oil and the CombiTitrant 2 Aquastar 1 ml/2 mg H_2O with one-component reagents (both from Merck Millipore, Billerica, USA). The titer was determined at least three times each day using a 1% water-standard (1 g/10 mg H_2O) (Apura, Merck Millipore, Billerica, USA).
All measurements using titration were carried out in triplicates.

Dynamic viscosity. An Anton Paar Rheometer (MCR 302, Anton Paar, Austria) equipped with a cone-plate geometry (50mm, 1° angle, gap 0.2mm) and a Peltier system (0–100 °C) was used to determine the dynamic viscosity. The temperature was set to 40 °C, and the measurements were performed at a shear rate of 100 s^{-1} with a constant sample volume of 0.8 ml. Measurements were carried out in triplicates.

Dielectric constant. A parallel plate type electrode was built with two stainless steel plates. The plates were fixed at a constant distance of 0.5 mm by 4 PTFE washers (Ø 4 mm) and suitable PTFE screws (12 mm in length). Each plate was equipped with a 150 mm stranded wire (cross-sectional area 1.5 mm^2) and connected to a precision LCR meter (4280A, Hewlett Packard). The capacitor was then placed in a sealed PTFE housing filled with the respective oil. The setup and the oil samples were tempered at 20 °C before analysis to ensure a constant and evenly distributed temperature. The variation of the oil

temperature during measurements was found to be less than 0.5 °C. The dielectric constant was determined by dividing the capacitance of the oil (C_x) by the capacitance of the air (C_0):

$$\varepsilon = \frac{C_x}{C_0} \quad (1)$$

All measurements were performed at 1 MHz and carried out in triplicates.

2.5 Oleogel analysis

Stock solution preparation. Stock solutions with varying mass fractions of sterol and sterol ester were prepared. Independently of the concentration for each analysis, the molar ratio of sterol: sterol ester was always 1:1 (40:60 mass ratio). The respective amounts were carefully weighed into glass beakers and heated to a maximum of 98 °C after the oil was added on a magnetic stirrer until fully dissolved.

Gel firmness. Freshly prepared 6 % w/w stock solutions were poured into glass Petri dishes (Ø 110 mm) up to a height of 15 mm, cooled to room temperature, and sealed with parafilm. Samples were stored at 5 °C for 7 days before firmness was determined using a static material testing machine (Zwick GmbH & Co. KG, Germany) equipped with a 0.5-inch cylindrical probe. After the preset force of 0.02 N was detected, the cylinder penetrated the sample to a depth of 3 mm, and the force-displacement motions were recorded by the associated program testExpertII. Each sample was penetrated five times, and the distance between each penetration point and the wall of the petri dish was always greater than 10mm.

Gel-sol transition. Differential scanning calorimetry was performed with a Netzsch 214 Polyma (Netzsch-Gerätebau GmbH, Selb, Germany). 10–15 mg of oleogel (16 % w/w structurant) was cut from the middle of each sample using a scalpel, weighed into aluminum pans, and hermetically sealed. After an isothermal period of 10 min at 20 °C, the samples were heated to 105 °C at a constant rate of 10 °C·min^{-1}. The gel-sol transition temperatures and enthalpies (ΔH_{tot}) were determined using Proteus® software (Netzsch-Gerätebau GmbH, Selb, Germany). Additionally, Gauss curves (ΔH_{peak}) were fitted in the thermograms using PeakFit software (Systat Software GmbH, Erkrath, Germany). The fitted peak represents the dissolution of tubes, which is then used to calculate the peak % of the total dissolution enthalpy [3]:

$$peak\% = \frac{\Delta H_{peak}}{\Delta H_{tot}} \cdot 100 \quad (2)$$

The measurements were carried out in triplicates.

Sol-gel transition and strain sweep. Sol-gel transition temperatures were determined via dynamic mechanical thermal analysis (DMTA) with a plate-plate geometry (gap 0.2mm). The upper plate was sandblasted to avoid slipping of the sample. Hot oleogel solutions (10 % w/w, 0.8 ml) were pipetted onto the preheated plate (80 °C). Subsequently, the solution was cooled from 80 to 10 °C at a fixed cooling rate of 5 °C/min. The measurements were performed within the LVE at a strain of 0.05 % and an angular frequency of 10 rad/s. The sol-gel transition temperature was calculated using the associated program (Rheoplus, Anton Paar, Austria). It is defined as the crossover of the loss (G") and storage modulus (G') upon cooling. All measurements were carried out in triplicates.
After gelation occurred, the samples were left to rest for 20 min at 20 °C. Then, a strain sweep was performed at 10 rad/s and 20 °C. The data was used to determine G'_{max} and the strain at which the sample starts to be irreversibly damaged (γ_{max}).

Atomic force microscopy (AFM). The network structure was visualized using atomic force microscopy (AFM). Therefore, the method proposed by Matheson, A. B.; Koutsos, V.; Dalkas, G.; Euston, S. and Clegg, P. was used with minor adaptions[19]. A small drop of the hot oleogel solution was applied on freshly cleaved mica sheets (16 % w/w sterols), placed in single-use Petri dishes, and stored at room temperature until gelation occurred. Once the samples were gelled, they were sealed with parafilm and stored at 5 °C for 7 days before analysis. Measurements were performed at the Department of Applied Physical Chemistry at the Technical University Berlin (Prof. Gradzielski) with a Cypher S (Asylum Research, Santa Barbara, CA) atomic force microscope operating in tapping mode. The instrument was equipped with OLYMPUS OMCL cantilevers (model AC160TS-R30, nominal tip radius 7 nm) with a spring

constant of 26 N/m and a resonance frequency of 300 kHz. All images were processed and edited using Gwyddion free software package [20].

Table 2 Overview of performed tests of oil and oleogel samples, all tests mentioned in this table were performed with purified canola (C), sunflower (S) and flaxseed oil (F), additive concentration was 1.0, 2.5 and 5.0 % w/w on oil, oleogels additionally contained 6, 12 or 16 % w/w of an equimolar mixture of phytosterol/γ-oryzanol

Analysis	**Additive**					**sample**	
	none	**18:1**	**toco**	**mono**	**H_2O**	**oil**	**oleogel**
PV	x	x	x	x	x	x	
Water content	x				x	x	
Free fatty acids	x	x	x	x	x	x	
Dielectric constant	x	x	x	x	x	x	
Dynamic viscosity	x	x	x	x	x	x	
Firmness	x	x	x	x	x		x
$T_{gel\text{-}sol}$ (DSC)	x	x	x	x	x		x
$T_{sol\text{-}gel}$ (Rheometer)	x	x	x	x	x		x
G'_{max} & strain	x	x	x	x	x		x
AFM	x	selected samples					x

3. Results and discussion

3.1 Chemical and physical characterization of oils

Table 2 provides an overview of the experiments performed, while Table 3 shows shows oil quality parameters before and after purification and after saturation with water. The first part of this study discussed the changes due to oil purification in-depth. Hence, in this part, only the alterations caused by the additives will be addressed.

Although plant oils are generally recognized as hydrophobic, they contain minute amounts of water. In refined oils, water is likely located in micelles formed by traces of amphiphilic molecules such as mono- and diglycerides and phospholipids. After the purification procedure, the oils almost exclusively comprise triacylglycerols, and thus water cannot be stabilized. However, the water content increased from 13-17 ppm to 80-120 ppm after the treatment at 90 % humidity for 48 h. Elevated temperatures, continuous airflow in the chamber, and the high humidity favor the formation of peroxides in oils with polyunsaturated fatty acids [21, 22]. Depending on the reaction path, water might be dissociated or formed. Interestingly, canola oil contains slightly more water than sunflower oil before purification and after exposure to high humidity, but less PV and no FFA. That implies the individuality of reaction paths during PV formation and a generally higher oxidative stability of canola oil. Nevertheless, the water content was still significantly lower after the humidity treatment when compared to natural oils.

Moreover, oil viscosity increased due to the treatment which is probably related to the formation of peroxides, radicals, and consequently free fatty acids. Reportedly, the continuous phase's viscosity has a crucial impact on the self-assembling process during oleogelation since it influences or reduces the sterol and the sterol ester's diffusion rate [3, 5]. Consequently, a higher bulk viscosity will impede diffusion and hamper the molecular stacking, which results in a delay of gelation. In general, the viscosity of TAG oils increases with aliphatic chain length, the absence of double bonds, and the content of minor polar components such as primary and secondary oxidation products [3]. Hence, oil viscosity decreased with IV and after eliminating minor components.

Table 3 Chemical and physical parameters of natural (-N), purified (-P) and moisturized (-H_2O) canola (C), sunflower (S) and flaxseed (F) oils: ε- dielectric constant, RI – refractive index, PV- peroxide value, ρ – density, η- dynamic viscosity, H_2O - water

Sample	ε [-]	n [-]	PV [meq/kg]	η [mPa·s]	H_2O [ppm]	FFA [mg/100g]
C-N	3.0576 ±0.002	1.4653 ±7.2·10^{-5}	4.5 ±0.1	33.2 ± 0.02	46.8.7 ±4.4	11.7 ± 0.4
C-P	3.0027 ±0.002	1.4557 ±3.1·10^{-5}	0.5 ±0.1	25.5 ±0.02	13.4 ±1.1	n.d.
C-H_2O	3.0489 ±0.003	1.4643 ±3.1·10^{-5}	0.9 ±0.2	29.2 ±0.03	88.6 ±2.4	n.d.
S-N	3.1825 ±0.001	1.4669 ±6.5·10^{-5}	26.6 ±3.4	30.4 ±0.05	224.0 ±8.7	75.3 ±2.3
S-P	3.0102 ±0.003	1.4582 ±4.9·10^{-5}	0.9 ±0.3	21.4 ±0.09	19.9 ±1.2	n.d.
S-H_2O	3.1799 ±0.005	1.4656 ±9.2·10^{-5}	25.5 ±1.6	27.6 ± 0.04	79.9 ±1.1	9.6 ±0.9
F-N	3.3129 ±0.001	1.4736 ±2.3·10^{-5}	30.2 ±2.9	25.1 ±0.01	326.4 ±11.3	84.4 ±1.8
F-P	3.2001 ±0.004	1.4662 ±8.2·10^{-5}	22.6 ±1.4	17.7 ±0.07	17.1 ±4.2	n.d.
F-H_2O	3.3097 ±0.001	1.4721 ±1.2·10^{-5}	84.9 ±5.7	22.9 ±0.07	121.7 ±14.7	17.9 ±1.6

Moreover, it was hypothesized that the FFA and PV content does not change by admixing, except after the humidity treatment since hydrolysis of TAGs and oxidation reactions might occur. Nevertheless, the FFA and PV content were determined for the highest additive concentration (5 % w/w) in oleic acid, tocopherol acetate, and monoglyceride samples. No significant changes could be observed (data not shown).

Table 4 shows the sol-gel and gel-sol transition temperatures, the dissolution enthalpy, firmness, and maximum storage modulus in the linear viscoelastic region of oleogels from purified oils. The results were discussed in the first part of this study [1]. Here, they serve as a reference for the data obtained for oleogels with additives. That enables a convenient visualization of whether admixing affects a specific parameter, the extent, and the direction of change (synergy or suppression).

Table 4 Sol-gel, gel-sol transition temperatures, dissolution enthalpy, firmness and maximum storage modulus of oleogels from purified oils without additives, 16 % w/w sterol/sterol ester 1:1 molar

sample	$T_{sol-gel}$ [°C]	$T_{gel-sol}$ [°C]	ΔH [J/g]	F_{max} [N]	G'_{max} [10^{-5} Pa·s]
C-P	29.1 ±0.1	80.5 ±0.2	6.49 ±0.08	27.5 ±0.36	3.38 ±0.01
S-P	30.2 ±0.4	79.7 ±0.6	6.49 ±0.19	27.1 ±0.30	3.47 ±0.01
F-P	30.5 ±0.7	77.1 ±0.4	6.62 ±0.06	25.8 ±0.37	3.47 ±0.02

It should be mentioned that oil permittivity was determined for all samples, but results are only shown for water-saturated samples (Table 3). However, in oil samples containing tocopherol acetate, only an insignificant dose-dependent decline of the permittivity was observed (ε~2.99 [23]). On the other hand, the permittivity of oleic acid at 20°C is approximately 2.28, and hence considerably lower than purified TAG oils [24–26]. In line with that, the permittivity decreased with increasing admixing of oleic acid in all three oils. The differences at 5 % w/w admixing were found to be -0.036, -0.037, and -0.046 for canola, sunflower, and flaxseed oil, respectively.

In contrast, the addition of monoglycerides reportedly increases solvent permittivity [25]. However, in samples containing 2.5 or 5 % w/w monoglycerides, the permittivity had to be measured at approximately 50 °C due to the formation of crystalline particles at lower temperatures. Hence, the absolute values can not be compared. The increase in permittivity relates to monoglycerides' functional groups, namely one ester and two hydroxyl groups. In combination with their hydrophobic FA tail, this renders them excellent surfactants able to act as hydrogen bond donors and acceptors.

Lowering the solvent permittivity (oleic acid) might result in a smaller fraction of dissolved oryzanol when network formation is completed. However, the carboxyl group of oleic acid can act as both a hydrogen bond donor (-OH hydroxyl group) and hydrogen bond acceptor (-C=O carbonyl group), potentially retarding oleogel formation or modifying the network properties or both. On the other hand, the ester group of tocopheryl acetate can only accept hydrogen bonds. Nevertheless, the chromane compound comprised of a phenyl group (aromatic) and tetrahydropyran (non-aromatic) might form weak interactions with the ferulic acid moiety like those participating in inter-fibril interactions [8].

3.2 Gel formation and dissolution

Reportedly, the continuous phase's viscosity has a crucial impact on the self-assembling process during oleogelation since it influences or reduces the sterol and the sterol ester's diffusion rate [3, 5]. Consequently, a higher bulk viscosity will impede diffusion and hamper the molecular stacking, which results in a delay of gelation. In general, the viscosity of TAG oils increases with aliphatic chain length, the absence of double bonds, and the content of minor polar components such as primary and secondary oxidation products [3]. Hence, oil viscosity decreased with IV and after eliminating minor components. Moreover, the humidity treatment had the opposite effect, which is possibly connected to the formation of oxidation products, as explained earlier.

Figure 3 shows the relative oil viscosity of purified canola, sunflower, and flaxseed oil with water (bottom right) or different concentrations of either monoglycerides (top right), oleic acid (top left), or tocopheryl acetate (bottom left). The addition of water and especially monoglycerides increased the viscosity. When admixing the monoglyceride mix, a linear dose-dependent response can be seen. On the other hand, the viscosity remains relatively constant for all levels of tocopheryl acetate and oleic acid. Consequently, a possible suppression of sol-gel transition in these samples is likely the result of interactions between

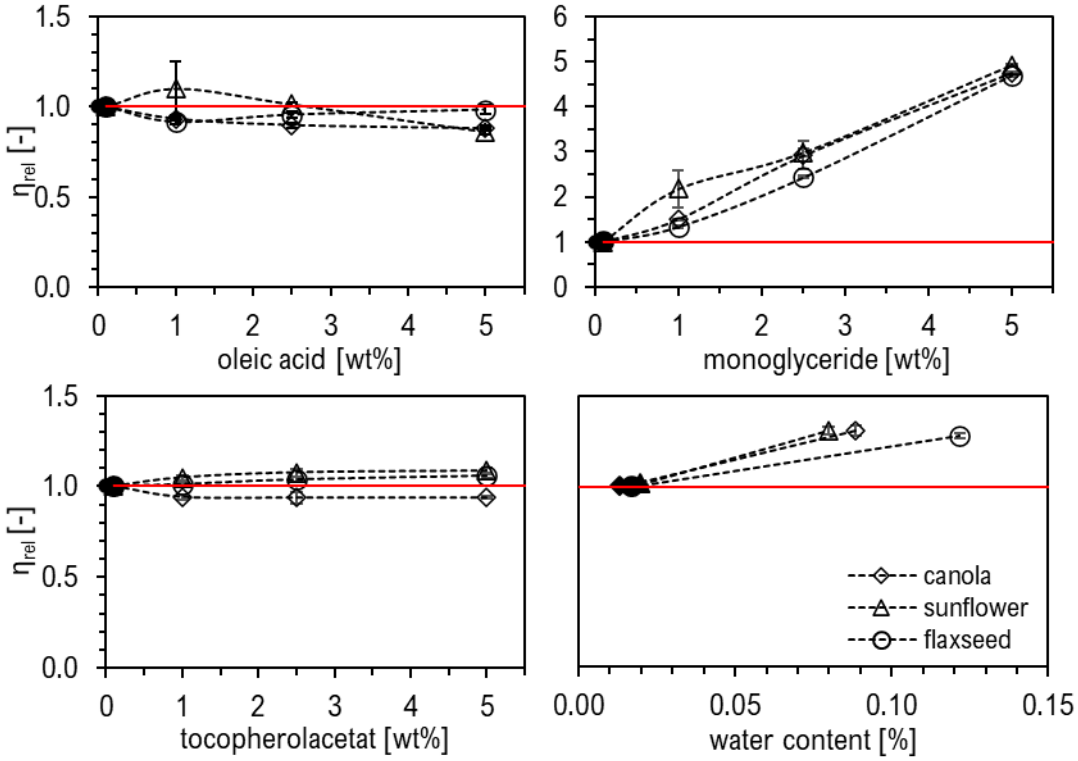

Figure 3 Relative viscosity at 40°C of purified canola, sunflower and flaxseed oil and with 1.0, 2.5 and 5.0 % w/w : oleic acid (top left), monoglyceride mix (top right), tocopheryl acetate (bottom left) and water (bottom right), lines to guide the eye

tocopheryl acetate or oleic acid with the ferulic acid moiety of γ-oryzanol. On the other hand, gel formation could be hampered in solvents with monoglycerides and water due to decreased diffusion rate caused by a greater viscosity.

Figure 4 depicts the relative sol-gel transition temperatures of oleogels determined by oscillatory rheometry (temperature sweep at low strain). The associated program *Rheoplus* calculated the temperature at the crossover of storage (G') and loss modulus (G"), representing the transition from a liquid to a semi-solid. It should be mentioned that the relative values of phase transitions (sol-gel and gel-sol) were always calculated by relating °C/°C instead of K/K.

The addition of minor components hinders the transition in all samples, and the effect increases with their concentration in most cases. However, the decline might rest on distinct effects: oleic acid and tocopheryl acetate interact with the sterols, thus retarding the self-assembling process. A similar effect has been reported for thermal degradation products [3]. A nearly linear dose-dependent decline of sol-gel temperature can be observed in samples with oleic acid (Figure 4, top left). In contrast, the retardation appears to be slightly inconsistent in samples containing tocopheryl acetate (Figure 4, bottom left). To

what extent the effect is related to the differences in interactions with the ferulic acid moiety or local concentration differences of the additive during the sol-gel transition can not be stated with certainty at this point.

In oils comprising monoglycerides, the high bulk viscosity impedes the structurants diffusion and lowers the probability of encountering. Therefore, network formation is significantly hampered (Figure 4, top right). The effect appears to level off above substitution levels of 2.5 % w/w. However, that is caused by the crystallization of monoglycerides, resulting in a rapid increase of G'. Hence, the crossover of G' and G" refers to the network formation of monoglyceride crystals. Besides, at concentrations below supersaturation (e.g., 1 % w/w), the fibril formation might be impeded due to hydrogen bond formation

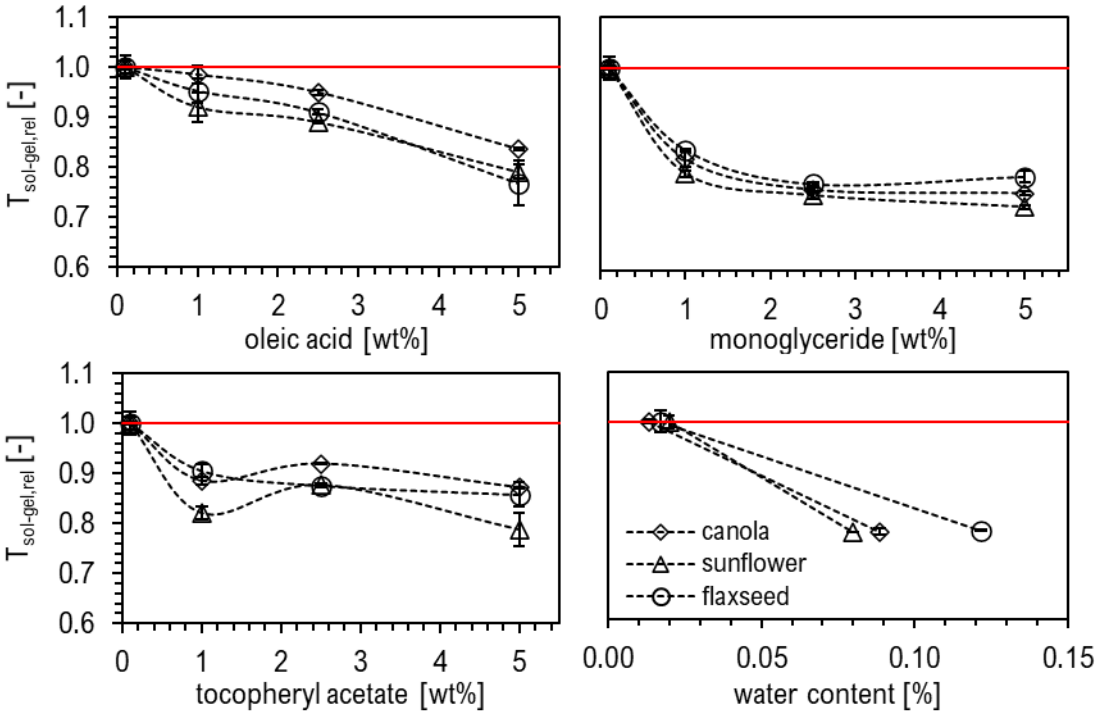

Figure 4 Sol-gel transition temperature of purified canola, sunflower and flaxseed oil oleogels (16 % w/w structurants) and with 1.0, 2.5 and 5.0 % w/w: oleic acid (top left), monoglyceride mix (top right), tocopheryl acetate (bottom left) and water (bottom right), lines to guide the eye

between the hydrophilic tale of monoglycerides and the ferulic acid moiety or the hydroxyl group of sitosterol. DSC thermograms and the determination of gel-sol transition temperatures might reveal whether the development of the fibrillar network actually occurred in these samples.

The humidity treatment increases the water content, viscosity, and peroxides in purified oils (Table 3), which likely suppresses network formation. Nevertheless, the amount of water in samples was marginal, and thus the decline in sol-gel transition is likely related to the bulk viscosity.

It is essential to be aware of the retardation of the sol-gel transition. In many food production processes, the fat's physical state during processing and in the final product is crucial. For example, during ice cream production, the fat should be liquid during premix production to enable small droplet sizes and solidify during ripening to provide stability.

Figure 5 shows the relative gel-sol transition temperatures of oleogels, determined by differential scanning calorimetry. The peak temperature can be associated with the dissolution of tubes, particularly the hydrogen bond break-up between sitosterol and oryzanol [3, 15]. Moreover, it relates to the number of tubules in the gel network, which correlates with the quantity of structurants and their solubility [16]. A lower solubility of structurants increases the number of tubes, and hence gel-sol transition temperatures supposedly increase.

Within each data set, all three oils follow the same trend when the additive concentration increases. Moreover, the admixing did not result in significant modifications of gel-sol transition temperatures, in line with previous data [3]. Nevertheless, the addition of monoglycerides led to the most pronounced decrease of the gel-sol transition temperatures. That is in line with the data shown in Figure 3 and 6. The increased continuous phase viscosity possibly causes the reduced sol-gel transition temperatures but

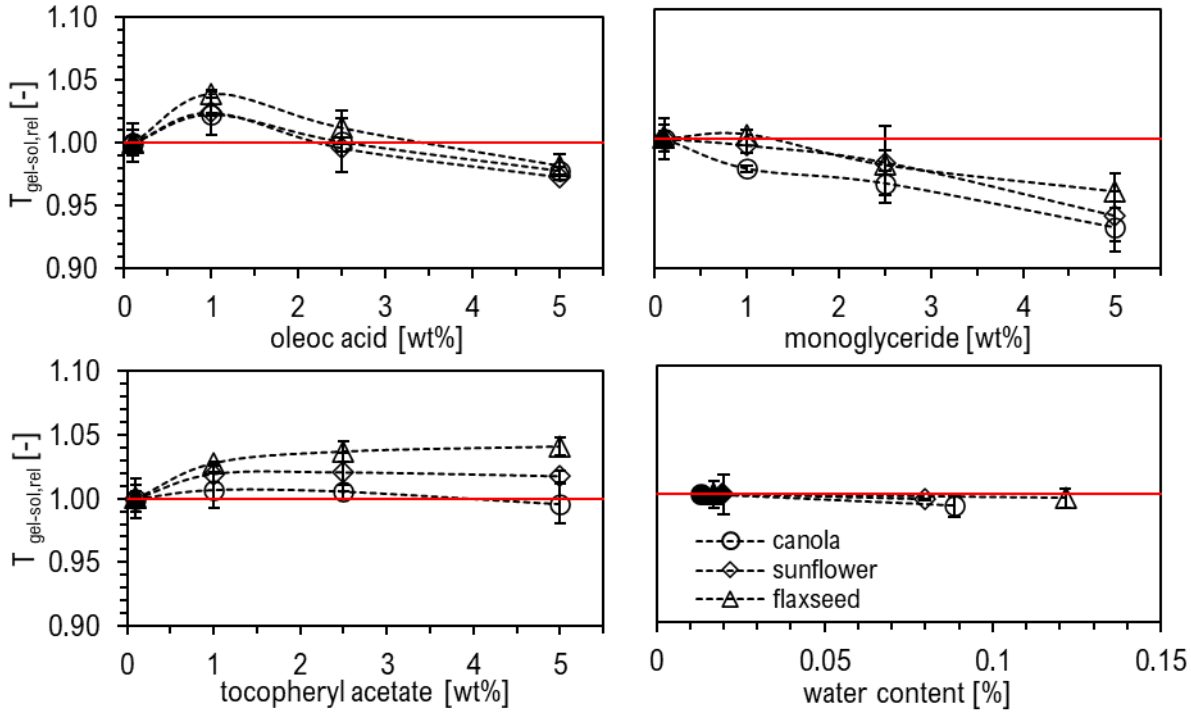

Figure 5 Relative gel-sol transition temperature of purified canola, sunflower and flaxseed oil oleogels (16 % w/w structurants) and with 1.0, 2.5 and 5.0 w% w/w: oleic acid (top left), monoglyceride mix (top right), tocopheryl acetate (bottom left) and water (bottom right), filled markers refer to gels without additives, lines to guide the eye

cannot explain the other effects observed. At monoglyceride concentrations of 2.5 and 5.0 % w/w, a second peak was observable in the DSC thermograms at 60 and 65 °C, respectively. However, careful assessment of the thermograms indicates more complex interactions between the monoglycerides and the oryzanol/sitosterol composition because of the evolution of the peaks. Hence, the ideal solubility curve of the monoglyceride mix was generated using its melting temperature (70.9 °C) and enthalpy (105.3 J/g), and average molecular mass (339.1 g/mol). From the curve, it was evident that the secondary peaks are not related to the dissolution of monoglyceride crystals since the transition temperatures derived from the solubility curve are much lower (<5 °C). However, the peak area and temperature of the second peak increased with increasing monoglyceride concentration (see Figure 7), and simultaneously the peak area and temperature of the fibril dissolution decreased. Hence, the second dissolution peak is likely a composite structure formed by the monoglyceride and either the sterol or the sterol ester similar to what has been reported for oryzanol and lecithin [11]. However, this structure's nature was not analyzed and will not be discussed within the scope of this work.

The water saturation led to a minor decrease in gel-sol transition temperatures. Possibly, the increase of permittivity caused by the formation of FFA, peroxides, and higher water content (Table 3) reduced the number of tubes in the network by slightly increasing oryzanol solubility. However, this can not be assessed conclusively.

Oleogels with oleic acid exhibit a different dose-dependent behavior: at lower concentrations, there seems to be an increase in the transition temperature, followed by a continuous decline. Although oleic acid hampers the network formation (Figure 4, top left), it seems that at low concentrations, the reduction of solvent permittivity and reduced solubility outbalance the delay once the gel development has finished and reaches equilibrium. At higher concentrations of oleic acid, this supporting effect inverts. As the permittivity increases (at high concentrations), the solubility effect might be canceled by an increased number of interactions formed preferentially between oleic acid and the ferulic acid moiety of oryzanol. Consequently, high levels of oleic acid might shield the sterols from forming tubules, and thus, the gel-sol transition temperature decreases. Still, the steps between the concentrations are relatively coarse, and thus no statement can be made whether there is a real maximum and at which concentration. Surprisingly, oleic acid and monoglyceride show linear dose-response with the same reduction of the gel-sol temperature per % additive in the range studied.

Finally, in gels containing tocopheryl acetate, gel-sol temperatures first increase at low substitution levels (1 % w/w). Further admixing (2.5 and 5.0 % w/w) does not seem to impact dissolution temperatures, and a plateau is reached. The increase seems to be more assertive in oils with a lower IV. It was mentioned earlier that tocopheryl acetate did not affect the permittivity of oils considerably. Hence, gel-sol transition temperatures should be invariant.
The detailed mechanisms leading to the effects observed cannot be unraveled at this point. However, the data on transition enthalpies, rheological properties, and microstructure of oleogels with additives provide additional information.
Surprisingly, the dissolution enthalpy was relatively constant for all levels of tocopheryl acetate (Figure 6, bottom left). That means that the amount of energy needed to break up the interactions within the oleogel network did not change in the presence of tocopheryl acetate. That is in line with results reported for oleogels from oils high in deterioration products [3]. However, that does not imply that the network interactions did not change by adding tocopheryl acetate. At this point, any interpretations on the modification of gel-sol transition enthalpy and temperature in the presence of tocopheryl acetate,

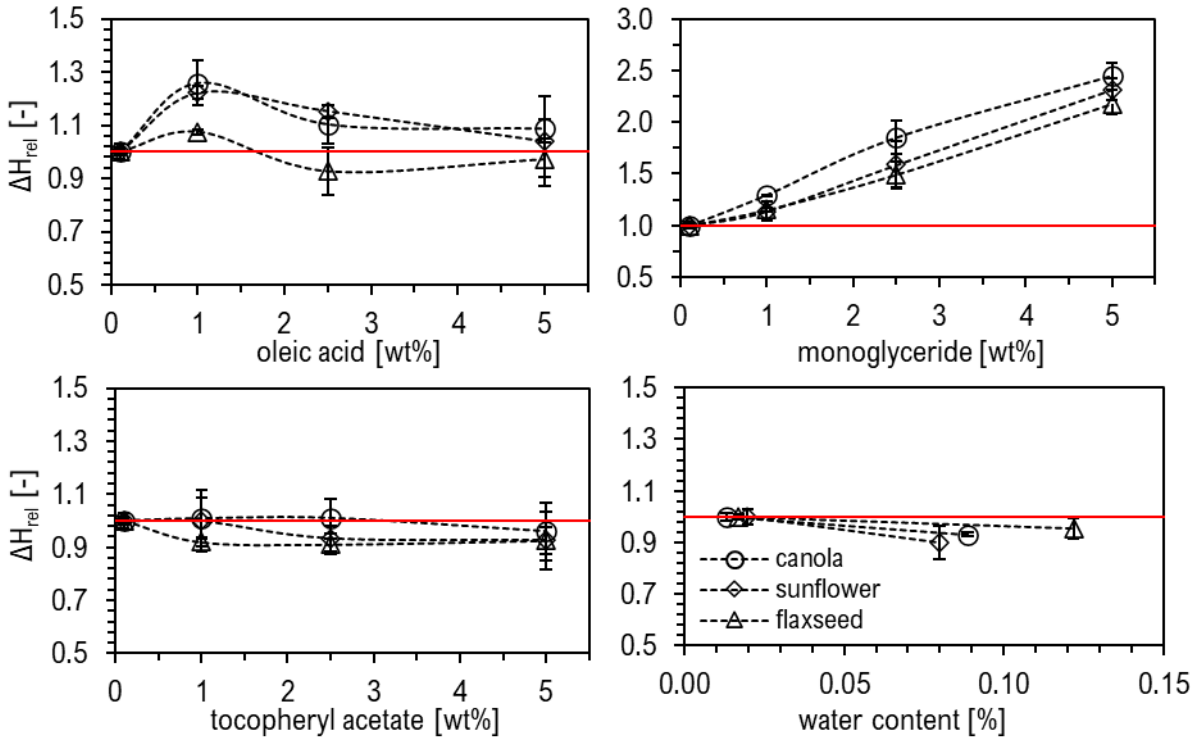

Figure 6 Relative enthalpy of dissolution of purified canola, sunflower and flaxseed oil oleogels (16 % w/w structurants) and with 1.0, 2.5 and 5.0 % w/w: : oleic acid (top left), monoglyceride mix (top right), tocopheryl acetate (bottom left) and water (bottom right), lines to guide the eye

unfortunately, suffer from inconsistency.
The transition enthalpy of oleogels with oleic acid seems to develop similarly to the gel-sol transition temperature, in line with the interpretation that more tubes might be present at a low substitution (1 % w/w) due to a reduced solubility. The amount of tubes is similar to purified oil oleogels for 2.5 % w/w and 5 % w/w samples since the gel dissolution energy does not vary substantially, taking the margin of error into account. That indicates that the gel's disintegration overall relates to the same energy, possibly due to contributions of tubules' dissolution and interactions of tubules and oleic acid. That could be related to oleic acids' flexibility to act as both a hydrogen bond donor and acceptor, enabling numerous connections with the structuring elements (Figure 1). In flaxseed oil oleogels, these interactions might not be available because oleic acid associates with primary oxidation products instead.
Not surprisingly, the dissolution enthalpy of monoglyceride oleogels increases linearly with monoglyceride concentration (Figure 6, top right). That is in the first instance the result of the formation of the composite structure discussed above. This identification of a dispersed solid monoglyceride phase should not be mistaken as an explanation for the viscosity increase, illustrated in Figure 3, since the

viscosity was determined at 40°C and hence above the dissolution temperature of the monoglyceride crystals.
The slight decrease in enthalpy in oleogels with water observed is in line with the previous findings.
Similar to the first part of this study, the DSC thermograms were used to disentangle the peak fronting from the actual peak area since it was found that the gel-sol transition process begins before the appearance of the peak [15, 27–29]. That was connected to the break-up of intra-tubule interactions (between individual fibrils), while the peak temperature relates to the dissolution of tubes (inter-tube interactions) [3]. One could argue that the peak fronting might be related to the gradual dissolution of tubes and that the break up of inter-and intra-tube bonds overlap in DSC thermograms.
However, a considerable increase of peak fronting was reported for samples with minor polar components. Simultaneously, the peak area decreased, causing a practically constant total dissolution enthalpy for all samples [3].
After fitting the peak area, the peak % was calculated according to Equation 2. It should be mentioned that most thermograms of flaxseed oleogels could not be adequately processed for peak fitting since peaks appeared broader and less sharp. Hence, the fit was often insufficiently defined, and results are considered less convincing. For the sake of completeness, they are still included in Figure 7. The data appear to be independent of the oil type if the flaxseed oleogel system results are ignored. For the addition of water, only a minute reduction is observed in line with the results reported for ΔH. (Figure 7, bottom right). The addition of monoglycerides has a dramatic effect on the relative peak area related to the tubule dissolution. Again this has to be interpreted with caution. The reduction shown is, after all, not only due to conversion from intra- to inter-tubular interactions but also caused by the additional contribution of the composite structure mentioned above. Still, when the data is adjusted for the dissolution of the secondary structure, a substantial reduction of the peak area is still found. Although no clear second peak was observable in DSC thermograms when 1 % w/w monoglycerides were added, the adjusted fibril dissolution area was lower than in the reference. That indicates that the composite structure formation occurs at additive concentrations as low as 1 % w/w, in line with the decrease in gel-sol transition temperatures.

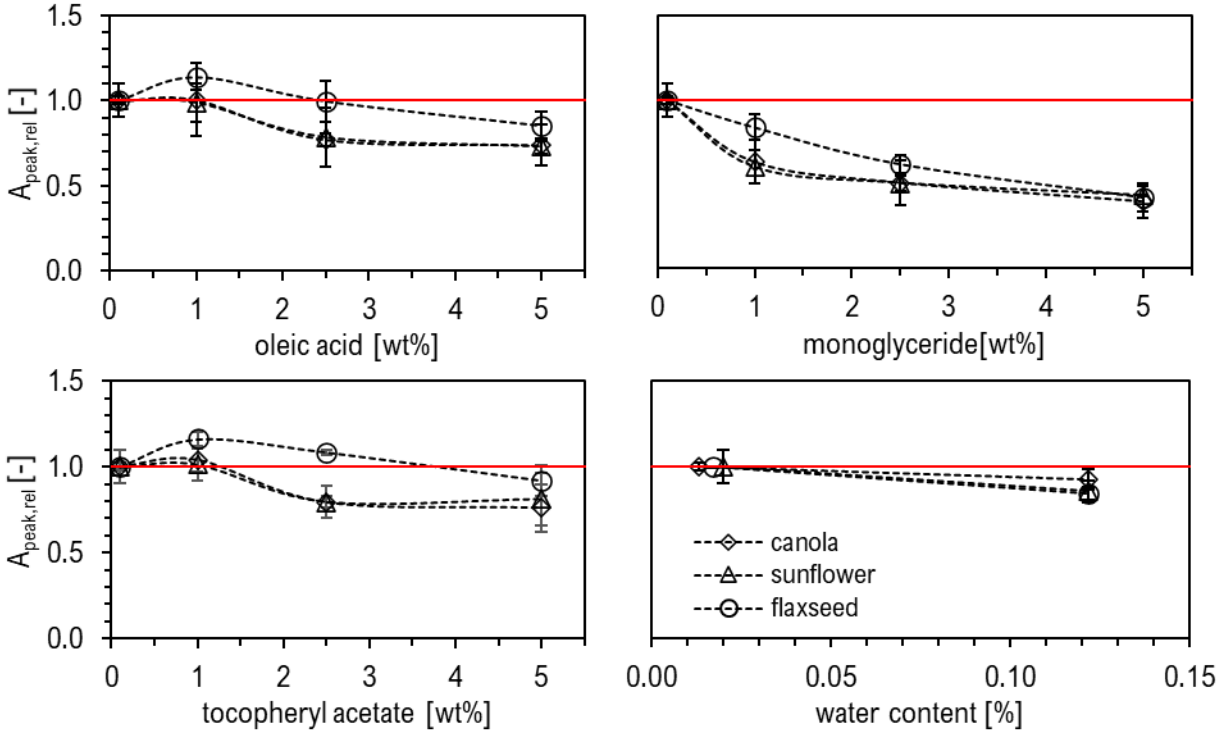

Figure 7 Relative peak area [-] determined for oleogels of purified canola, sunflower and flaxseed oil oleogels (16 % w/w structurants) and with 1.0, 2.5 and 5.0 % w/w : oleic acid (top left), monoglyceride mix (top right), tocopheryl acetate (bottom left) and water (bottom right), lines

The samples containing oleic acid or tocopheryl acetate show a different picture. In both cases, the peak area appears to remains unchanged on the inclusion of 1 % w/w of the additive. For the inclusion levels

of 2.5 and 5.0 % w/w, a reduction of 20 to 25 % of the enthalpy contribution of the primary peak related to tubule dissolution was identified. Here, the underlying mechanism is believed to be driven by the contribution of changes in solubilities and concurrent interaction shifts.

For these systems, the peak area decreases in favor of peak fronting, which has been assigned to a shift from intra- to inter-tube interactions. Oleic acid might accumulate on the tube surface by forming hydrogen bonds with functional groups of the ferulic acid moiety (Figure 1), thus blocking connections responsible for fibril-fibril interactions. Hence, the type of bond possibly shifts but does not necessarily generate inter-tubular connections. However, the mechanistic interpretation is more complicated for the samples containing tocopheryl acetate due to the nature of the molecule. Nevertheless, the results show that higher substitution levels (2.5 % w/w and above) result in a shift from intra to inter-tube interactions in tocopheryl acetate and oleic acid samples. In monoglyceride and water samples, the decline was associated with the reduction of tubes in line with the reduced dissolution temperatures.

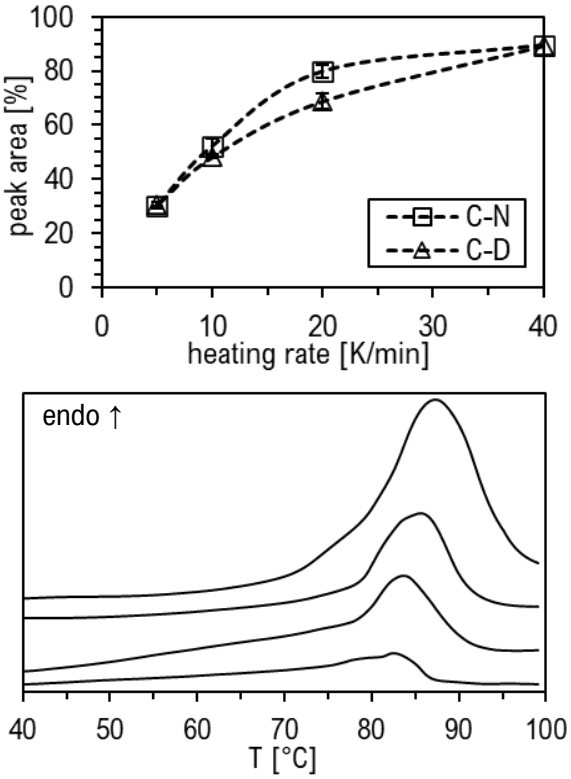

Figure 8 Top: peak area % of oleogels (16 % w/w structurants) with natural canola (C-N) and deteriorated canola oil (C-D) in dependence DSC scanning rate. Bottom: exemplary DSC thermograms scanned with 40, 20, 10 and 5 K (from top to bottom), curves shifted for clarity, similar thermograms were obtained for oleogels from deteriorated oil

One could raise the question, whether connecting the peak area to fibril dissolution is legitimate. To justify this assumption, oleogel samples produced with either natural (small fronting) or deteriorated (large fronting) canola oil. These were subjected to DSC heating programs with varying scan rates (5, 10, 20, and 40 K/min). Subsequently, the relative peak areas % were calculated. Figure 8 top depicts that the calculated peak areas increase considerably with the heating rate and converge towards a threshold value (~90%). For the lowest and highest scan rates (5 and 40 K/min), no significant difference in peak areas between C-N and C-D could be identified. That renders these rates inappropriate for the differentiation of energy contributions. Figure 8 bottom shows that the signal for 5 K/min is shallow and that the peak can hardly be distinguished from the fronting.

In general, the solubility of a solute is increasing with temperature for any dissolution process. In a two-phase system containing a dispersed phase of either a solid crystalline or a less defined self-assembled structure, the dispersed phase volume is reduced monotonously on temperature increase to yield a value of zero at the dissolution temperature. The gel-sol transition temperature is, per definition, lower because the critical aggregation dispersed phase volume is greater than zero at this point. However, the scan rates used for dissolution studies (DSC) are not zero, and consequently, kinetic effects are superimposed on the equilibrium disintegration characteristics of the dispersed phase. The approach applied here and described previously [2] builds on the observation that for the sitosterol/oryzanol structuring system, typical segregation of the melting thermogram occurs at intermediate scan rates. There are two phenomena assigned to the thermograms, the break up of inter-tubular bonds, relating to the ferulic acid moieties, and the actual disintegration of the self-assembled tubules (intra-tubular). The inter-tubular interaction, which might overlap with the ferulic acid moiety interactions, is more sparsely distributed in space and hence less hampered by transport phenomena. It is assumed to proceed continuously, here referred to as fronting. In contrast, the continuous dissolution of the fibril structure is assumed to be slow compared to the intermediate scan rates. That results in relatively rapid disintegration of the tubules once the dissolution temperature has been reached, causing a distinct peak. Figure 8 illustrates that at

low scan rates, probably both disintegration processes proceed gradually and overlap. At high scan rates, both processes trail the temperature increase and proceed rapidly at temperatures above the dissolution temperature. Although this interpretation is not verified, the consistency of the results obtained justifies the approach for the time being.
In summary, distinct effects can be seen for the additives. Monoglycerides partially canceled out the development of the fibril network by increasing solvent viscosity and forming a composite structure. Due to the very low solubility of water in purified oils, the effect on gel-sol transition temperatures was marginal, indicating a similar amount of tubes in the gel. However, sol-gel transition temperatures decreased considerably, suggesting enhanced interactions of water and primary oxidation products formed during the humidity treatment with the structurants. Samples containing oleic acid and tocopheryl acetate seem to alter the network's interactions, leading to a shift from intra- to inter fibril connections, or an analog connection of ferulic acid moieties with the additives, which increased the fronting. The following section attempts to connect these findings to the macroscopic properties of oleogels.

3.3 Mechanical oleogel properties

Figure 9 shows the relative firmness of oleogels (16 % w/w) from purified canola, sunflower, and flaxseed oil with additives. In monoglyceride oleogels, a sharp decrease in firmness is observable at low concentrations, followed by an increase at 2.5 and 5.0 % w/w. A high viscosity reportedly hampers the formation of the sterol/sterol ester network as described elsewhere [5], causing the firmness reduction. However, at higher monoglyceride concentrations, 2.5 and 5 % w/w, the coexisting network of monoglycerides crystals contributes to increasing oleogel firmness. The initial decrease is less pronounced in flaxseed oil oleogels due to a lower solvent viscosity resulting in slightly more fibrils and bundles (see Figure 5, top right). The synergistic effect found for combinations of monostearate or monopalmitate and ethylcellulose in oleogels [30] could not be found for the mixed system studied here. In oleogels with oleic acid, canola, sunflower, and flaxseed oil show different trends at the lowest concentration (1.0 % w/w). While the network hardness seems slightly enhanced when sunflower oil is used, it appears unchanged in flaxseed oil oleogels and declines remarkably for canola oil oleogels. There is a gradual decrease for all three oil types at higher concentrations, which complies with the gel-sol transition temperature and the number of tubes in the network. Remarkably, in gels containing 5 % w/w oleic acid, the hardness decreased by 75, 62, and 54 % for canola, sunflower, and flaxseed oil, respectively. The bulk viscosity was unchanged for all concentrations (Figure 3). Simultaneously, the gel-sol transition temperature exhibited a maximum at 1 % w/w (+2-3% of the initial value), was equal to the initial value at 2.5 % w/w, and about 2.5 % lower at 5 % w/w (Figure 5). Hence, it is fair to assume that the shift from intra to inter-fibril interactions expressed in the relative peak areas (Figure 7) is less a contribution of strengthened bundeling. Even though a shift away from intra-firilar interaction occurs the association of the ferulic acid moeitiy with oleic acid does not seem to contribute to network strength but rather suppress intermolecular interactions. Consequently, this configuration considerably weakened the compression hardness of these oleogels. Although most refined oils usually do not contain FFAs, hydrolysis is a common degradation reaction in edible oils, and this study shows that even small concentrations alternate the oleogels' macroscopic properties considerably.

When added at low concentrations, tocopheryl acetate shows a synergistic effect on the firmness of oleogels for all three oils (Figure 9, bottom right). At higher concentrations of (2.5 and 5.0 % w/w),

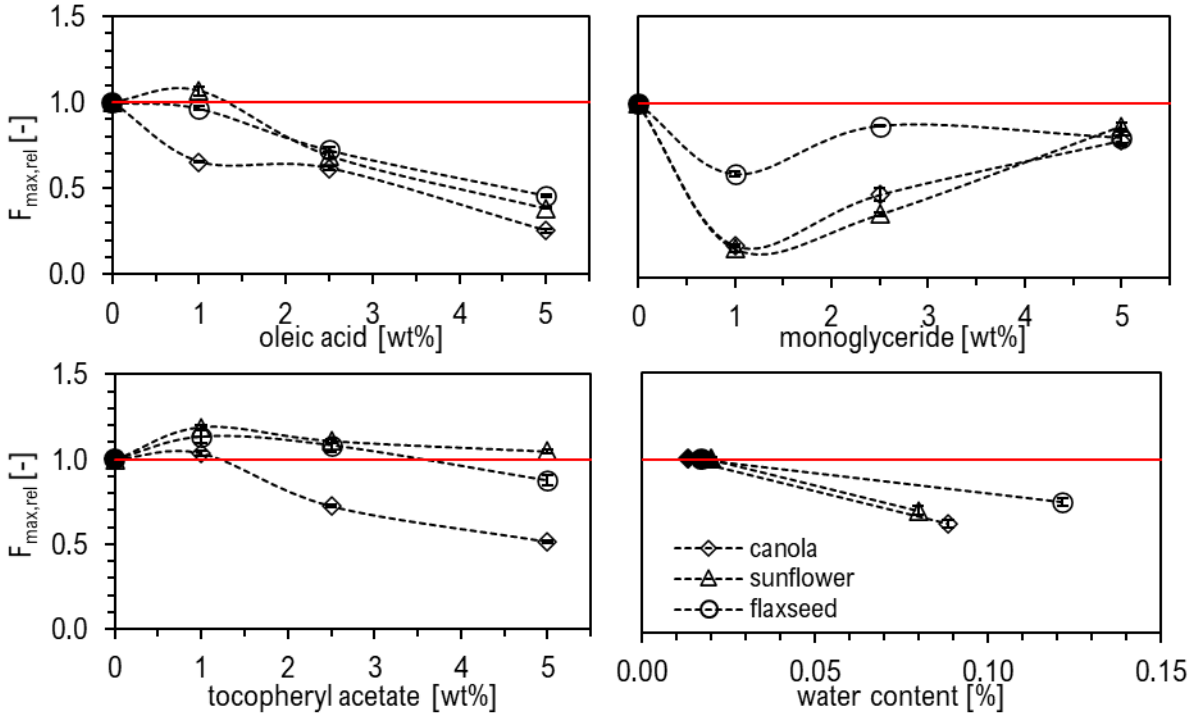

Figure 9 Firmness of purified canola, sunflower and flaxseed oil oleogels (16 % w/w structurants) and with 1.0, 2.5 and 5.0 % w/w : oleic acid (top left), monoglyceride mix (top right), tocopheryl acetate (bottom left) and water (bottom right), red line indicates initial firmness, dashed lines to guide the eye

firmness decreases, whereas the decline is most significant in canola oil. Like oleic acid, tocopheryl acetate did not change solvent viscosity, and the peak area % was unchanged for 1 % w/w and declined continuously at higher substitution. However, gel-sol transition temperatures were considerably higher for canola and sunflower oil and similar to the starting value in flaxseed oil oleogels. Therefore, a supportive effect on gel firmness is suggested at low concentrations. However, results appear inconsistent for the oils used since the higher amount of tubes indicated by a higher gel-sol transition temperature did not result in an overall firmer gel network. That might be related to a similar shift in interactions reported for oleic acid. However, interactions of scaffolding elements with tocopheryl acetate are likely different due to different interaction points and the difference in molecular size (Figure 1).

The firmness of water containing oleogels decreased significantly (Figure 10, bottom right) in line with the results of gel-sol transitions, indicating potentially fewer tubes present. Again flaxseed does not match the other oils' overlapping data, which might be due to the sensitivity of the flaxseed oil during sample preparation. Nevertheless, it is interesting to note that reduction of the gel-sol transition temperature by 0.3-2% corresponds to a network that is 25-37 % less hard. MD simulations of sitosterol/oryzanol in water indicated that water forms hydrogen bonds with the carbonyl group of oryzanol and the hydroxyl group of sitosterol [4]. Unfortunately, it remains unclear whether the water is causing the reduction since it is unclear if it is available for interactions or encapsulated in purified oils. Nevertheless, during the humidity treatment, the formation of oxidation products is stimulated (Table 3), and the impact of tube reduction and shift of interactions due to minor polar components likely overlap. It is hence impossible to relate the reduction of gel-sol transition temperature comprehensively to the decrease of oleogel firmness. Moreover, other parameters such as increased solvent viscosity (monoglycerides) impair this approach as well. That renders the gel firmness a vital parameter describing the networks' properties. Still, it does not allow for a detailed description of the changes in network arrangement induced by minor polar components.

Besides penetration and back extrusion tests, gels' deformation characteristics can be assessed using large deformation rheology such as amplitude sweeps. The results provide more detailed information about network properties and their breakdown characteristics. A gel's behavior under increasing strain is crucial for successful product development since most food production processes involve shearing.

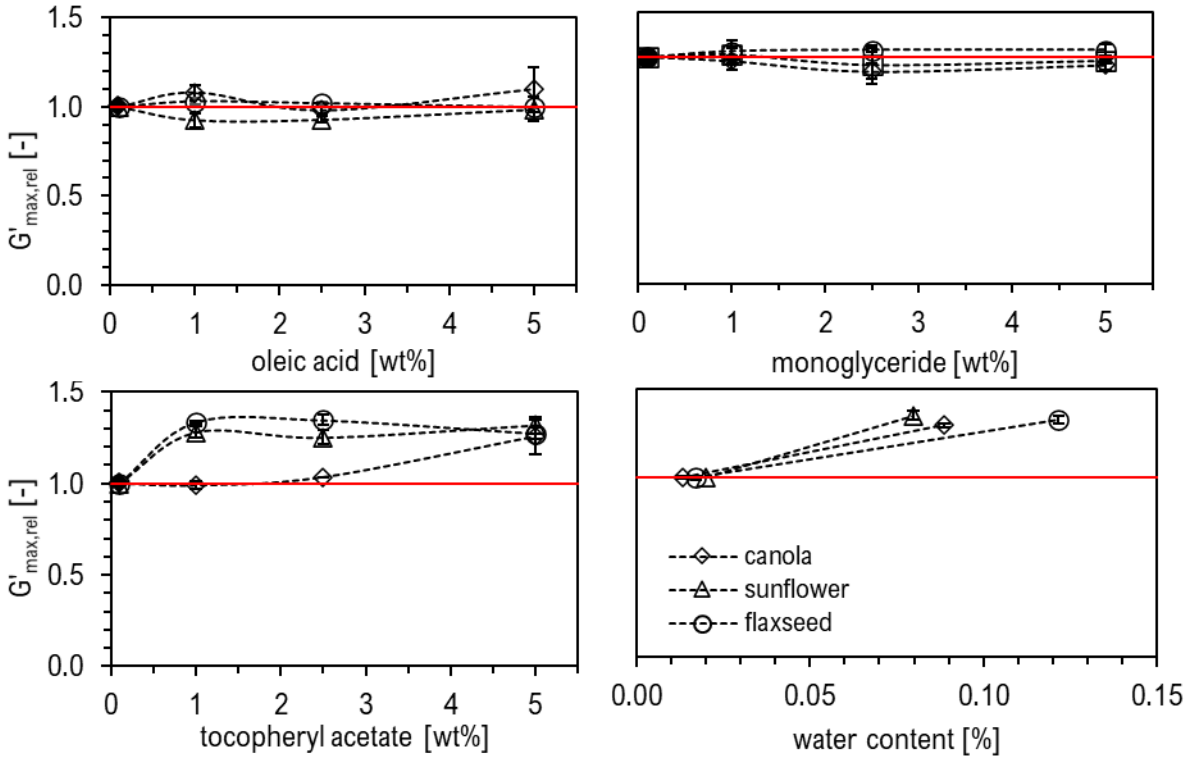

Figure 10 Relative maximum storage modulus (G' max) at 20°C of purified canola, sunflower and flaxseed oil oleogels (16 % w/w structurants) and with 1.0, 2.5 and 5.0 % w/w : oleic acid (top left), monoglyceride mix (top right), tocopheryl acetate (bottom left) and water (bottom right), red line indicates initial value of purified oil oleogels

An exemplary curve obtained by amplitude sweeps of sitosterol/oryzanol oleogels is given elsewhere [3]. Briefly, within the linear viscoelastic region (LVE), the maximum storage modulus (G'_{max}) can be determined. G'_{max} provides information about the gels' ability to store deformation energy and is directly related to the extent of cross-linking in the network but not necessarily to compression hardness [31]. As the strain increases, brittle fracturing occurs in the sample (for gels $\gamma_{max} \approx 0.5$ % [31]), indicating a gradual breakdown of the structure. Subsequently, the viscous behavior dominates, and the sample starts to flow at G'=G" (flow point). Reportedly, natural minor oil components and deterioration products increased G'_{max} compared to results obtained with purified oils [32]. Moreover, γ_{max} decreased, indicating that the network exhibited more connection points, which broke up more easily when subjected to stress. The same trend was detected in this study, where γ_{max} decreased continuously in all samples on additive inclusion (results not shown).

It is in the first place remarkable that the general trends in G' max do not correspond with those displayed in Figure 9 for F max. This illustrates again how difficult it is to define relevant characteristics for oleogels and formulate comprehensive interpretations [33]. Surprisingly, reducing the amount of tubes in the network and the concurrent monoglyceride network seem to cancel out and no changes in network connection points could be observed (Figure 10, top right). Although the same trend was observed for all oleic acid concentrations (Figure 10, top left), it is likely related to distinct effects. At low concentrations (1 % w/w), there seem to be slightly more tubes in the gel (Figure 5), and oleic acid molecules likely distribute on their surface, potentially interacting with the ferulic acid moiety. However, the amount seems to be insufficient to affect the extent of cross-linking in the network significantly. In contrast, at higher concentrations, G'_{max} remains unchanged, but the amount of fibrils is reduced (Figure 5). Hence, network connection points increase due to additional interactions of the carbonyl group of oleic acid resulting in an equal number of network junction zones. However, the results of gel firmness show that this network is not necessarily more stable against compression.

In oleogels containing tocopheryl acetate, G'_{max} exhibits the same trend observed for the hardness. While there is fewer cross-linking in canola oil oleogels (softest gel), in sunflower and flaxseed oleogels, G'_{max} increased up to 32 %. Nevertheless, the effect is most likely related to the greater amount of scaffolding elements in these samples, indicated by a higher gel-sol transition temperature (2-4% increase, Figure 5). Like oleic acid, this does not automatically result in harder gels (Figure 9). The observations are likely related to the differences in interactions of oleic acid and tocopheryl acetate with the tubules. However, any further details on the interactions cannot be answered within this study.
In the samples subjected to the humidity treatment, crosslinks increased by 29, 35, and 32 % for canola, sunflower, and flaxseed oil, respectively. Potentially, oxidation products and water accumulated on the surface of tubes and provide additional connection points that surprisingly do not increase hardness. Since water-saturated sunflower and flaxseed contained more primary oxidation products, the G'_{max} is possibly higher than in canola oil samples.
Distinct changes of macroscopic oleogel properties were observed considering the additives' different functional groups due to different interactions with scaffolding elements. However, at this point, it is unclear whether the differences observed in gel-sol transition temperatures (more or fewer tubes), firmness (amount of tubes and their arrangement), and network connection points (arrangement) result in visible changes in the network arrangement. To this end, atomic force microscopy was used to visualize the network surface of selected oleogel samples.

3.4 Microstructure of oleogels

Figure 11 shows AFM micrographs (10 µm scanning size) of selected canola oil oleogel samples. The top two rows show micrographs of samples containing 1 (top) or 5 % w/w oleic acid, tocopheryl acetate, and monoglycerides (from left to right), respectively. The bottom three pictures depict a gel from

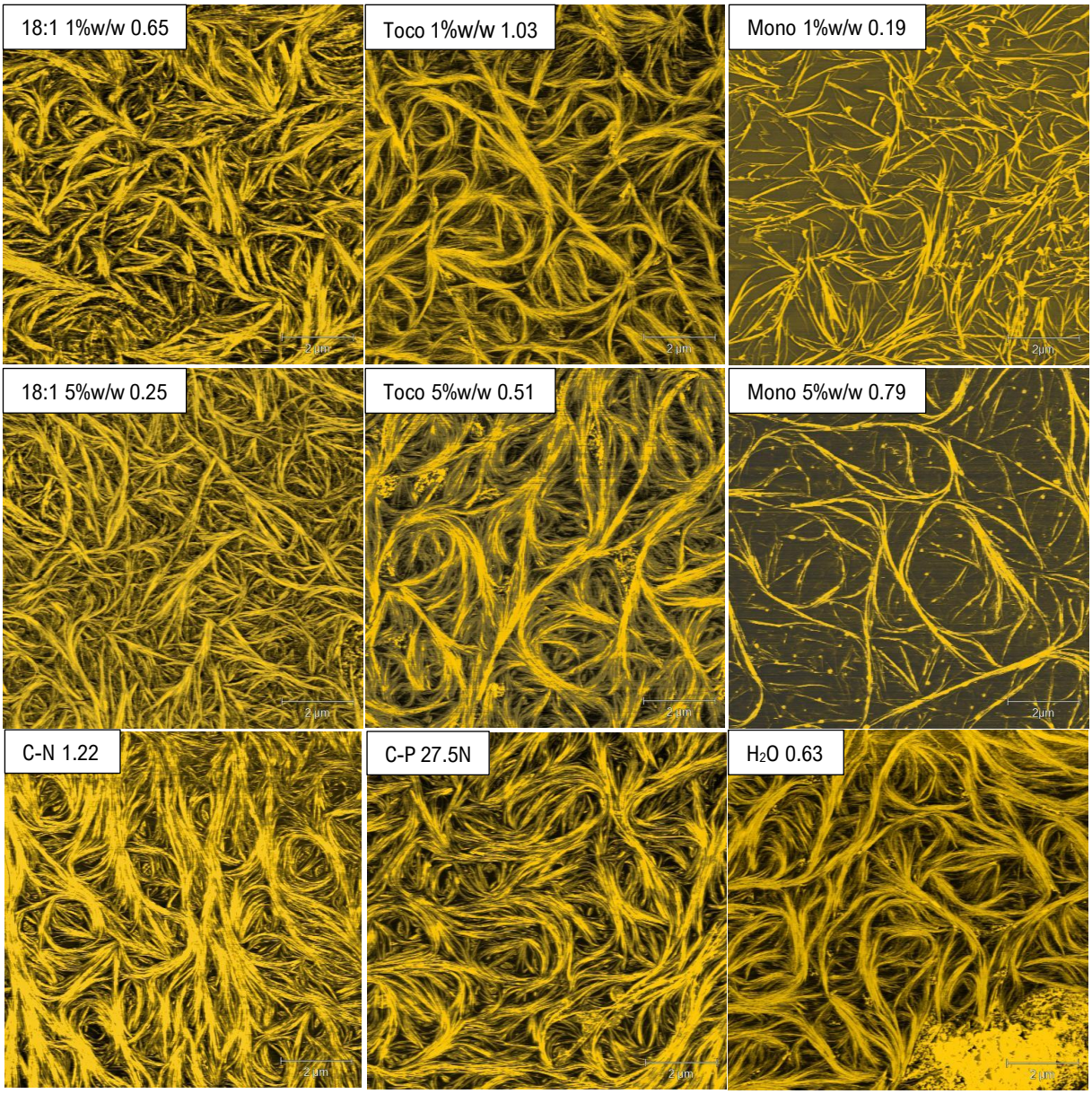

Figure 11 AFM-micrographs of canola oil oleogels with (16 % w/w structurants), top left croner shows additive, concentration (if applicable) and relative hardness, hardness related to purified canola oil (3rd row middle), scanning size 10µm, scale bar = 2µm

untreated canola oil (C-N, left), purified canola oil (reference, C-P, middle), and the gel after humidity treatment of the oil (H_2O, right). Moreover, in the top left corner of every image, the relative gel hardness is depicted, which was obtained by relating the respective force to that of the samples with purified canola oil. Fibrous structures are observable in all pictures, although their amount, alignment, and branching appear noticeably different.

In the sample comprising untreated canola oil (bottom left), the surface is packed with bundles that are twisted and align and exhibit numerous intersections. Similar results have been described in other studies [3, 4, 8]. Micrographs of oleogels from untreated sunflower and flaxseed oil showed very similar arrangements. Oleogels from purified oils reportedly exhibit large tubule alignment areas resulting in thick bundles, although the range of bundle sizes was considerably variable [1].

It was mentioned repeatedly that molecules forming similar interactions as those responsible for inter-tube interactions might accumulate on the tubule surface due to weak interactions. Moreover, they might block the stacking of sitosterol and oryzanol by forming strong hydrogen bonds like, for example, water and sitosterol.

In contrast, in samples containing monoglycerides, tube formation is impeded by the tremendous increase of solvent viscosity and the formation of a composite structure. The micrographs (Figure 11,

row 1 and 2, right) show a network of thinner bundles in line with that. Additionally, the amount of tubes seems to decrease with increasing monoglyceride concentration, and small spherical structures can be seen in both samples, glued to the bundle surface. Perhaps, the hybrid structure accumulates on the surface of tubes. Although these structures' existence was observable in DSC thermograms, their nature can not be determined with certainty at this point.
In gels containing 1 % w/w tocopheryl acetate (Figure 11, row 1 and 2, middle), the bundles appear slightly thinner but exhibit more extended areas of alignment than in the reference. That potentially results in a greater surface of the scaffolding elements, leading to a harder network. In contrast, in the sample with 5 % w/w tocopheryl acetate, bundles appear thicker. However, gel hardness was about 50 % less than for the sample with 1 % w/w. The findings agree to some extent with a recent publication studying the influence of solvent polarity on sterol/ sterol ester oleogels [14]. Based on SEM images, the authors hypothesized that bundles with large segments of alignments promote the gels' hardness. However, SEM is sensitive to artifacts since the intensive sample preparation might cause alterations in the network structure. Moreover, the authors used edible oils without any further characterization or standardization and did not consider other solvent-related effects on gel firmness, such as viscosity. Nevertheless, micrographs of sunflower oil oleogel appear almost identical to samples containing tocopheryl acetate, indicating that the structure of bundles (alignment and thickness) considerably influences the gels' resistance to, e.g., compression.
A different picture emerges in gels with oleic acid. In both samples, the bundles appear shorter and less twisted, while at the higher concentration, they are considerably thinner than at 1 % w/w. Considering the very low compression hardness, long, aligned bundles potentially result in more rigid gels. Surprisingly the sample comprising 5 % w/w oleic acid gave a very sharp image, although it was hypothesized that softer gels are harder to visualize due to low tip-sample interactions. Hypothetically, in the presence of oleic acid, the network structure was extensively exposed by the ethanol treatment. Indeed, the samples consistently showed a thin oil film on the surface, indicating the network's insufficient oil binding capacity.
The network arrangement of samples subjected to the humidity treatment appears similar to that of the reference, although bundles appear slightly thinner. They twist and turn as they approach each other. Consequently, any effects on gel hardness might be due to a reduction in the number of tubes, which can not be quantified using AFM, but was observed in gel-sol transition temperatures. It needs to be mentioned that the structure observable in the bottom right corner is an artifact due to low tip-sample interactions. Similar to samples containing oleic acid, an oil film formed on the sample surface, suggesting a lower oil binding capacity.
The illustration of the surface revealed significant changes in network arrangement regarding the type of polar additives and their concentrations. Nevertheless, AFM can not deliver factual information about the spatial distribution of the scaffolding elements. Although, due to that, interpretations remain somewhat imprecise, it appears that bundles with larger areas of alignment produce harder gels. Moreover, very thick bundles are not preferred since they lower the overall structuring surface of the network. In conclusion, it remains challenging to formulate a comprehensive interpretation that links the network's visualization with the properties discussed in the other sections of this manuscript.

4. Conclusion

This study provides new insights into the influence of selected polar minor components on sterol/sterol ester oleogels. Regarding the results presented in the first part [1], it is assumed that the impact of the FAs composition of triglycerides is negligible compared to the influence of minor polar components. Distinct effects were found regarding the type and concentration of the additive used. Although the purification of oils resulted in almost pure triglycerides, the formation of primary oxidation products during oleogel preparation can not be excluded, mostly in oils with a higher IV. That is reflected in somewhat larger deviations obtained in, for example, oleogel firmness, gel-sol transition temperatures,

and G'_{max}. Hence, the effects are, to some extent, the results of the superimposition of the bulk solvents' characteristics, such as polarity and viscosity, which are unavoidable.
However, all additives impeded the gel formation. That was associated with two distinct effects, which might overlap depending on the type of additive. On the one hand, weak interactions form between the functional groups of the structurants and the additives (oleic acid and tocopheryl acetate), retarding the molecular self-assembly. On the other hand, solvent viscosity hampers the rate of diffusion and thus the probability of encountering in monoglyceride samples. Moreover, a composite structure of monoglyceride and the sterol/ sterol ester system forms at the addition of 2.5 and 5.0 % w/w. This structure reduces the amount of fibrils in the gel indicated by a lower enthalpy and dissolution temperature. Indeed, in AFM micrographs, fewer bundles were visible. However, on the bundles, small clusters appeared, which seemed to be glued to their surface.
Nevertheless, hypothetical statements on the individual interactions of the additives' were made based on their functional groups. Consequently, potential interaction points with the sterol and sterol ester and the fibrils they form were identified. Regarding the findings of MD simulations, suggesting a shift of inter-tube interactions in highly polar solvents, a similar change was proposed for low concentrations of polar molecules and supported by DSC and AFM results. Different effects were observed regarding the additives' molecular structure, concentration, and whether or not other system parameters such as viscosity were altered.
A dose-dependent response similar to oils containing deterioration products occurred in samples containing tocopheryl acetate and oleic acid. The gel hardness was highest at low concentrations and declined as the concentration increased. Interestingly, the storage modulus in the LVE increased substantially with tocopheryl acetate. At the same time, it was relatively constant for all concentrations of oleic acid. That implies that the behavior is related to the physicochemical type of binding sites of the individual molecular species. Oleic acid and tocopheryl acetate both can accept a hydrogen-bond at their carbonyl group (–C=O). However, oleic acid is also a hydrogen-bond donor (–OH). Hence, the interaction between individual oleic acid molecules might outweigh the tendency to interact with oryzanol's ferulic acid moiety at high concentrations. However, this hypothesis is speculative and can not be substantiated at this point.
The networks' microstructure was considerably modified in gels containing either monoglycerides, oleic acid, or tocopheryl acetate. The latter showed thinner, straighter bundles at low concentrations (1 % w/w) with longer segments of parallel alignment compared to the reference. Since these samples were firmer, it was assumed that thinner, straighter bundles result in increased resistance to compression.
In line with that, firmness was reduced by 50 % in samples containing 5 % w/w tocopheryl acetate due to thicker bundles. The results are in good agreement with SEM micrographs of a recent study evaluating the influence of solvent polarity on sterol/sterol ester oleogels [14]. Potentially, there is a critical bundle size providing balancing contradictory effects of structuring surface and resistance to compression. However, with recent imaging technologies, any determinations lack expressiveness for the reasons mentioned. Hence, AFM should be interpreted carefully since micrographs only depict the surface, and sample-tip interactions are subjected to the success of oil removal from the surface. Nevertheless, fundamental changes of network structure due to minor polar components were visualized.
The influence of the humidity treatment on the microstructure appeared insignificant, which is likely related to the small amount of water dissolved in purified oils and the formation of primary oxidation products at the same time.
A different picture emerges in samples with oleic acid, where bundles appeared shorter yet thicker, associated with a softer network structure. The impression of a space-filling network could arise in the sample containing 5 % w/w oleic acid due to the high bundle density observable in AFM micrographs. However, that could relate to the ethanol treatment before the measurement, potentially removing more oil from the surface. Thus, studying the oil binding capacity of oleogels with additives would be an exciting addition to the presented structure assessment. A recently developed method determining oil perfusion showed good oil binding capacity of sterol/sterol ester oleogels [34].
Moreover, MD simulations of a triglyceride solvent containing varying concentrations of selected additives would be beneficial to provide additional information on the potential interactions suggested in this study. These could help verify or falsify the statement that low concentrations of additives actually

stabilize the structure studied here. How far these studies can help to elucidate the mechanism behind the effects observed once concentrations increase remains questionable. Previous studies, however, indicated that the number of hydrogen bonds formed between a polar molecule and the fibril during the simulation is a reliable indicator of the tube's stability. However, it remains unresolved to which extent solubility effects in highly polar solvents play a compensating role [4, 8].

In summary, the solvent composition, particularly minor polar components, substantially influence oleogel formation, network properties, and appearance. No drastic effects on gelator solubility can be expected in the range of concentrations studied. However, polar molecules can change inter-fibril interactions and network appearance substantially depending on their type and concentration. Significant variations in macroscopic gel properties such as hardness and maximum storage modulus were found on the addition of the polar components. Unfortunately, they did not correspond with one another. Nevertheless, the additives retarded network formation due to solute-solute interactions. Hence, it is crucial to pay close attention to the continuous phase's composition to understand and predict these effects. Therefore, a comprehensive characterization of the oils, such as fatty acid composition, minor components composition and concentration, and state of oil deterioration, is required. Only then comparability of different studies on oleogelation can be achieved, allowing for substantiated product development guidelines.

References

1. Scharfe M, Prange D, Flöter E (2021) The composition of edible oils modifies β-sitosterol/γ-oryzanol oleogels. Part I: Purified triglyceride oils. In preparation
2. Bot A, Flöter E (2018) Edible Oil Oleogels Based on Self-assembled β-Sitosterol + γ-Oryzanol Tubules. In: Edible Oleogels. Elsevier, pp 31–63
3. Scharfe M, Ahmane Y, Seilert J et al. (2019) On the effect of minor oil components on β-sitosterol/γ-oryzanol oleogels. Eur J Lipid Sci Technol. https://doi.org/10.1002/ejlt.201800487
4. Matheson A, Dalkas G, Mears R et al. (2018) Stable emulsions of droplets in a solid edible organogel matrix. Soft Matter 14:2044–2051. https://doi.org/10.1039/c8sm00169c
5. Calligaris S, Mirolo G, Da Pieve S et al. (2014) Effect of Oil Type on Formation, Structure and Thermal Properties of γ-oryzanol and β-sitosterol-Based Organogels. Food Biophysics 9:69–75. https://doi.org/10.1007/s11483-013-9318-z
6. Sawalha H, den Adel R, Venema P et al. (2012) Organogel-emulsions with mixtures of β-sitosterol and γ-oryzanol: influence of water activity and type of oil phase on gelling capability. J Agric Food Chem 60:3462–3470. https://doi.org/10.1021/jf300313f
7. Sawalha H, Margry G, den Adel R et al. (2013) The influence of the type of oil phase on the self-assembly process of γ-oryzanol + β-sitosterol tubules in organogel systems. Eur J Lipid Sci Technol 115:295–300. https://doi.org/10.1002/ejlt.201100395
8. Dalkas G, Matheson AB, Vass H et al. (2018) Molecular Interactions behind the Self-Assembly and Microstructure of Mixed Sterol Organogels. Langmuir 34:8629–8638. https://doi.org/10.1021/acs.langmuir.8b01208
9. Bot A, Gilbert EP, Bouwman WG et al. (2012) Elucidation of density profile of self-assembled sitosterol + oryzanol tubules with small-angle neutron scattering. Faraday Discuss 158:223. https://doi.org/10.1039/c2fd20020a
10. Cuevas MA, Shinzat RE, Costa MC et al. (2011) Gamma-oryzanol Solubility and Effect of Solvents Mixture. International Congress of Food and Engineering:1–3
11. Matheson AB, Dalkas G, Gromov A et al. (2017) The development of phytosterol-lecithin mixed micelles and organogels. Food Funct 8:4547–4554. https://doi.org/10.1039/c7fo01271c
12. Bot A, Veldhuizen YS, den Adel R et al. (2009) Non-TAG structuring of edible oils and emulsions. Food Hydrocolloids 23:1184–1189. https://doi.org/10.1016/j.foodhyd.2008.06.009
13. Lubosch K (2015) Weiterführende Untersuchungen Organogelbasierter Emulsionen am Beispiel eines Eiscreme-Premixes. Diplomarbeit, Technische Universität

14. Sawalha H, Venema P, Bot A et al. (2020) Effects of Oil Type on Sterol-Based Organogels and Emulsions. Food Biophysics. https://doi.org/10.1007/s11483-020-09654-8
15. Bot A, den Adel R, Roijers EC (2008) Fibrils of γ-Oryzanol + β-Sitosterol in Edible Oil Organogels. J Am Oil Chem Soc 85:1127–1134. https://doi.org/10.1007/s11746-008-1298-7
16. Bot A, Agterof WGM (2006) Structuring of edible oils by mixtures of γ-oryzanol with β-sitosterol or related phytosterols. J Am Oil Chem Soc 83:513–521. https://doi.org/10.1007/s11746-006-1234-7
17. Lampi A-M, Kamal-Eldin A (1998) Effect of α- and γ-tocopherols on thermal polymerization of purified high-oleic sunflower triacylglycerols. J Amer Oil Chem Soc 75:1699–1703. https://doi.org/10.1007/s11746-998-0319-x
18. Mariod A, Matthäus B, Hussein IH (2011) Effect of Stripping Methods on the Oxidative Stability of Three Unconventional Oils. J Am Oil Chem Soc 88:603–609. https://doi.org/10.1007/s11746-010-1703-x
19. Matheson AB, Koutsos V, Dalkas G et al. (2017) The microstructure of β-sitosterol: γ-oryzanol edible organogels. Langmuir 33
20. Nečas D, Klapetek P (2012) Gwyddion: An open-source software for SPM data analysis. Open Physics 10:99. https://doi.org/10.2478/s11534-011-0096-2
21. Choe E, Min DB (2006) Mechanisms and Factors for Edible Oil Oxidation. Comprehensive Reviews in Food Science and Food Safety:169–186
22. Partanen R, Raula J, Seppänen R et al. (2008) Effect of relative humidity on oxidation of flaxseed oil in spray dried whey protein emulsions. J Agric Food Chem 56:5717–5722. https://doi.org/10.1021/jf8005849
23. Szwajczak E, Świergiel J, Stagraczyński R et al. (2009) Viscous and dielectric properties of α -tocopherol and α -tocopherol acetate. Physics and Chemistry of Liquids 47:460–466. https://doi.org/10.1080/00319100902737455
24. Sousa FF de, Moreira SGC, Da dos Santos Silva SJ et al. (2009) Dielectric Properties of Oleic Acid in Liquid Phase. j bionanosci 3:139–142. https://doi.org/10.1166/jbns.2009.1013
25. Woo Y, Kim M-J, Lee J (2019) Prediction of oxidative stability in bulk oils using dielectric constant changes. Food Chemistry 279:216–222. https://doi.org/10.1016/j.foodchem.2018.12.012
26. Lizhi H, Toyoda K, Ihara I (2008) Dielectric properties of edible oils and fatty acids as a function of frequency, temperature, moisture and composition. Journal of Food Engineering 88:151–158. https://doi.org/10.1016/j.jfoodeng.2007.12.035
27. Bot A, den Adel R, Roijers EC et al. (2009) Effect of Sterol Type on Structure of Tubules in Sterol + γ-Oryzanol-Based Organogels. Food Biophysics 4:266–272. https://doi.org/10.1007/s11483-009-9124-9
28. den Adel R, Heussen PCM, Bot A (2010) Effect of water on self-assembled tubules in β-sitosterol + γ-oryzanol-based organogels. J Phys.: Conf Ser 247:12025. https://doi.org/10.1088/1742-6596/247/1/012025
29. Rogers MA, Bot A, Lam RSH et al. (2010) Multicomponent hollow tubules formed using phytosterol and gamma-oryzanol-based compounds: an understanding of their molecular embrace. J Phys Chem A 114:8278–8285. https://doi.org/10.1021/jp104101k
30. Lopez-Martínez A, Charó-Alonso MA, Marangoni AG et al. (2015) Monoglyceride organogels developed in vegetable oil with and without ethylcellulose. Food Research International 72:37–46. https://doi.org/10.1016/j.foodres.2015.03.019
31. Mezger TG (2016) Das Rheologie Handbuch: Für Anwender von Rotations- und Oszillations-Rheometern. FARBE UND LACK // BIBLIOTHEK. Vincentz Network, Hannover
32. Scharfe M (2019) On the importance of minor components and oil properties for oleogel strength, Sevilla
33. Flöter E, Wettlaufer T, Conty V et al. (2021) Oleogels - Their Applicability and Methods of Characterization: under review. Molecules
34. Theierl S (2021) On the application of oleogels in savoury products. Master Thesis, TU Berlin